analytical chemistry

pubs.acs.org/ac Article

Rapid and Quantitative *In Vitro* Evaluation of SARS-CoV-2 Neutralizing Antibodies and Nanobodies

Weishu Wu,[○] Xiaotian Tan,[○] Jennifer Zupancic, John S. Schardt, Alec A. Desai, Matthew D. Smith, Jie Zhang, Liangzhi Xie, Maung Khaing Oo, Peter M. Tessier,* and Xudong Fan*

Cite This: *Anal. Chem.* 2022, 94, 4504−4512 Read Online

ACCESS | Metrics & More | Article Recommendations | Supporting Information

ABSTRACT: Neutralizing monoclonal antibodies and nanobodies have shown promising results as potential therapeutic agents for COVID-19. Identifying such antibodies and nanobodies requires evaluating the neutralization activity of a large number of lead molecules *via* biological assays, such as the virus neutralization test (VNT). These assays are typically time-consuming and demanding on-lab facilities. Here, we present a rapid and quantitative assay that evaluates the neutralizing efficacy of an antibody or nanobody within 1.5 h, does not require BSL-2 facilities, and consumes only 8 μL of a low concentration (ng/mL) sample for each assay run. We tested the human angiotensin-converting enzyme 2 (ACE2) binding inhibition efficacy of seven antibodies and eight nanobodies and verified that the IC_{50} values of our assay are comparable with those from SARS-CoV-2 pseudovirus neutralization tests. We also found that our assay could evaluate the neutralizing efficacy against three widespread SARS-CoV-2 variants. We observed increased affinity of these variants for ACE2, including the β and γ variants. Finally, we demonstrated that our assay enables the rapid identification of an immune-evasive mutation of the SARS-CoV-2 spike protein, utilizing a set of nanobodies with known binding epitopes.

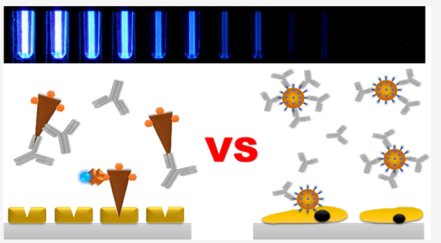

INTRODUCTION

COVID-19 poses a threat to human health and has a huge societal impact. In the past 2 years, millions have died of the disease.[1,2] In the battle against COVID-19, monoclonal neutralizing antibodies and nanobodies have been explored as therapeutic agents that can prevent severe symptoms for infected patients, potentially saving millions of lives. To date, pharmaceutical companies such as Regeneron and Eli Lilly have developed neutralizing monoclonal antibody products that proved to have therapeutic efficacy against COVID-19.[3] However, there are key challenges related to screening for neutralizing antibodies and nanobodies. Virus neutralization assays (VNAs) are currently the gold standard for *in vitro* evaluation of neutralizing antibodies.[4,5] However, such neutralization assays need to be performed in Biosafety Level 3 (BSL-3) laboratories, whereas their safer replacement, pseudovirus neutralization assays (pVNAs), requires BSL-2 facilities.[6] Live virus and pseudovirus neutralization assays take 2−4 days to complete. The safety concerns and long assay times drastically limit accessibility and throughput for neutralizing antibody evaluation. On the other hand, high-throughput immunoassays such as those based on surface plasmon resonance[7] or sandwiched enzyme-linked immunosorbent assays (ELISAs)[8−10] can be used to examine the binding capability and affinity between antibodies and the SARS-CoV-2 spike protein. However, they cannot differentiate the neutralizing antibodies from binding but non-neutralizing antibodies. Therefore, a fast and accessible assay to screen neutralization activities of antibodies is highly desired.

Here, we present a rapid (<90 min; see Figure S1) assay for screening of potential neutralizing antibodies and nanobodies based on the competitive inhibition of SARS-CoV-2 spike protein interaction with the extracellular domain of the human angiotensin-converting enzyme 2 (ACE2). In this study, we tested and compared four different versions of the SARS-CoV-2 spike proteins, *i.e.*, the receptor-binding domain (RBD), the S1 subunit, the S-extracellular domain (S-ECD, including the S1 subunit and the extracellular region of S2 subunit) monomer, and the S-ECD homotrimer, and evaluated the feasibility of our assay with seven SARS-CoV-2 spike RBD-specific monoclonal antibodies. We found that the S-ECD homotrimer can generate the most comparable results with SARS-CoV-2 pVNAs. With this approach, we successfully identified monoclonal antibodies and nanobody Fc fusions, with potent inhibition activity against the wild-type SARS-CoV-2 spike protein. We further examined the inhibitory activity of these antibodies and nanobodies against three widespread SARS-CoV-2 variants. Our results show that the

Received: January 5, 2022
Accepted: February 22, 2022
Published: March 3, 2022

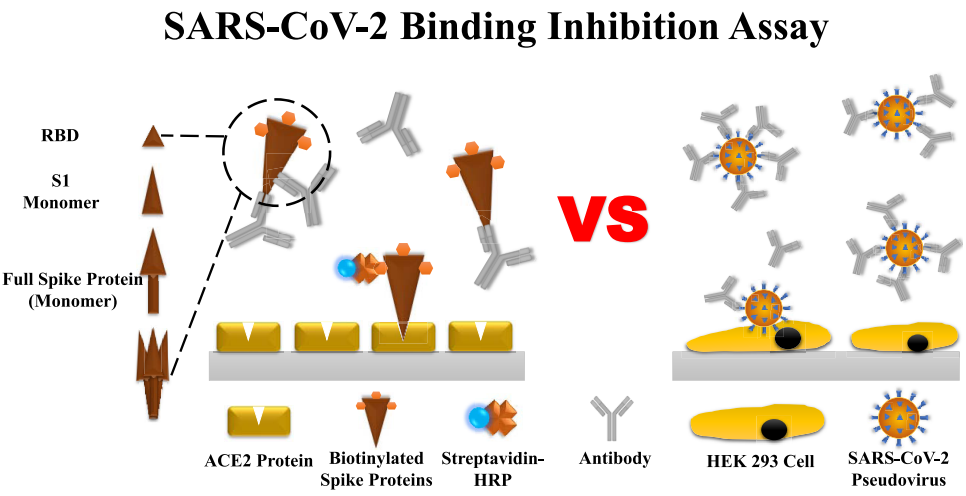

Figure 1. Schematic of the rapid *in vitro* inhibition assay (RIVIA, left panel) and pseudovirus neutralization assay (pVNA) using HEK 293 cells (right panel).

inhibition activities decrease significantly in many antibodies and nanobodies, but some of these agents maintain nearly the same inhibition activities, suggesting that their binding epitopes may be less affected by prevalent RBD mutations and thus can potentially be used as broader neutralizers against SARS-CoV-2 variants.

MATERIALS AND METHODS

Assay System. The assays run on an Xpress ELISA system whose detailed description is reported in previous publications and patents.[11−13] In brief, the disposable cartridge is made of polystyrene through injection molding and consists of 12 microfluidic assay reactors (800 μm in diameter), each of which requires only 8 μL of sample or reagent. In each step, the drawing and withdrawing of sample or reagent were controlled by a multichannel pump and can be completed within 1 s.

Materials. 1× PBS buffer (DY006), 10% BSA buffer (SLBR9934V), and wash buffer concentrate (WA126) were purchased from R&D Systems. Streptavidin Poly-HRP (PI21140), Poly-HRP dilution buffer (ENN500), the chemiluminescence substrate (SuperSignal ELISA Femto Substrate, 37075), distilled water (UltraPure DNase/RNase-free, 10977023), and SuperBlock (PBS) buffer (37515) were purchased from Thermo Fisher.

Human recombinant ACE2 protein (hFc Tag, 10108-H02H), SARS-CoV-2 (2019-nCoV), spike RBD-His recombinant protein (40592-V08H), and SARS-CoV spike/S1 protein (S1 subunit, His-tag, 40150-V08B1) were provided by Sino Biological. Recombinant SARS-CoV-2 spike His protein (10549-CV), recombinant SARS-CoV-2 spike GCN4-IZ His protein (10561-CV), recombinant SARS-CoV-2 B.1.351 spike GCN4-IZ His protein (10786-CV), recombinant SARS-CoV-2 B.1.1.7 spike GCN4-IZ His protein (10796-CV), and recombinant SARS-CoV-2 P.1 spike GCN4-IZ His-tag protein (10795-CV) were purchased from R&D Systems. The trimerization for the four S-ECD homotrimers is achieved using the GCN4-IZ trimerization tag. Biotinylation was accomplished using EZ-link NHS-PEG4-biotin (21330) from Thermo Fisher.

Humanized chimeric antibody D006 (40150-D006), neutralizing antibody MM43 (mouse mAb, 40591-MM43), MM57 (mouse mAb, 40592-MM57), and neutralizing antibody R001 (rabbit mAb, 40592-R001) were provided by Sino Biological. Anti-SARS-CoV-2 spike RBD neutralizing antibody human IgG3 (AS35) was purchased from Acro Biosystems (SAD-S35). Neutralizing antibody CB6 (human)[14] and CR3022 (human)[15] were reported previously and subsequently expressed and purified in-house by the Tessier group at the University of Michigan for the assays.

Nanobody Fc fusions KC3.ep3,[16,17] Ty1,[18] VHH-72,[19] and the Nb series[20] were reported to exhibit neutralizing abilities against the SARS-CoV-2 virus. The ones tested in the assays were all expressed as bivalent Fc fusions and purified by the Tessier group.

Lenti-X Concentrator (631232) and Lenti-X 293T cells (632180) were purchased from Takara. Luciferase substrate (E6110) was from Promega ONE-Glo.

Reactor Preparation. As illustrated in Figure S1, ACE2 was first immobilized on the active inner surface of the reactors. The working solution of ACE2 was in 1× PBS (pH 7.4) at 4 μg/mL. After this, two consecutive blocking steps (2.5% BSA, then Superblock) were used to reduce the noise level. After each of the steps mentioned above, a washing step was followed. A 1× wash buffer was used by diluting the wash buffer concentrate in UltraPure DNase/RNase-free distilled water.

Assay Protocols. A conceptual illustration of the assay is shown in Figure 1. Details of the protocols, including incubation time, can be found in Figure S1. The working solution for samples was a blocking buffer (2.5% BSA), which was prepared by diluting 10% BSA in 1× PBS.

Tenfold serial-diluted antibody solutions starting at 50 μg/mL were mixed with specific concentrations of biotinylated S proteins and left at room temperature to react. The biotinylated RBD, S1 subunit, S-ECD monomer, and S-ECD homotrimer concentrations were 20, 100, 70, and 70 ng/mL, respectively. These concentrations were chosen to produce comparable and strong chemiluminescence intensity under the same conditions in the absence of antibodies or nanobodies. Then, the antibody and S protein mixture's reacted solution was drawn into the reactors to react with ACE2 immobilized on the reactor's inner surface. For the detection steps, 2000× diluted Poly-HRP solution was used, followed by the chemiluminescence substrate. With current market prices, the cost for performing one trial of RIVIA (12 channels per trial

https://doi.org/10.1021/acs.analchem.2c00062
Anal. Chem. 2022, 94, 4504−4512

for each antibody) is less than $15, including the cost of ACE2, the S-ECD homotrimer, streptavidin Poly-HRP, and the chemiluminescence substrate.

Signal Reading and Data Processing. After the final step, a CMOS camera was used to read the chemiluminescence signal. A multiple-exposure approach[21] was used to increase the dynamic range. The signal is normalized to that obtained with 3 s of exposure time. The binding inhibition rates in RIVIA are calculated using the following formula: $\left(1 - \frac{\text{signal intensity}}{\text{baseline}}\right) \times 100\%$. The baseline is calculated as the averaged signal intensity for the control channels where antibody concentrations are 0 μg/mL. The IC_{50}, half-maximal inhibitory concentration, from RIVIA is calculated by linear fitting of the data points in the linear regime that are at the proximity of the half-inhibition concentration. For the convenience of data presentation on linear-log scale figures, for all antibodies and nanobodies, the baseline measurements (0 ng/mL) are marked as 0.1 ng/mL on the X-axis, in all relevant figures.

Pseudovirus Neutralization Assays. SARS-CoV-2 pseudovirus neutralization assays were conducted following previous reports.[17,22−24] For pseudovirus particle preparation, Lenti-X 293T cells were seeded at 6×10^5 per well in 6-well plates in RPMI media containing 10% fetal bovine serum (FBS) and 1% penicillin/streptomycin (P/S) and cultured at 37 °C with 5% CO_2 until cells reached 50−70% confluency. Cells were transfected with lipofectamine 2000 and the following third-generation lentiviral plasmid system: (1) HDM-Hgpm2 plasmid (BEI number NR-52517) encoding HIV Gag-Pol under CMV promoter (0.22 μg), (2) HDM-tat1b plasmid (BEI number NR-52518) encoding HIV Tat under CMV promoter (0.22 μg), (3) pRC-CMV-Rev1b plasmid (BEI number NR-52519) encoding HIV Rev (0.22 μg), (4) pHAGE-CMV-Luc2-IRES-ZsGreen-W (BEI number NR-52516) lentiviral transfer plasmid encoding the coexpression of luciferase and ZsGreen (1.00 μg), and (5) pCMV3 SARS-CoV-2 S untagged delta 19AA C-term plasmid encoding the SARS-CoV-2 spike (S) protein with a 19-amino acid deletion at the C-terminus (0.34 μg). At 24 h post transfection, the medium was changed to fresh RPMI with 10% FBS and 1% P/S. To harvest SARS-CoV-2 pseudovirus particles, the cell supernatant was collected and passed through a 0.45 μm filter 72 h post transfection. Pseudovirus particles were then concentrated using a Lenti-X Concentrator following the manufacturer's protocol with a 4 °C overnight incubation at the incubation step. The virus pellet was resuspended in a volume of 50 μL of Opti-MEM per well of virus harvest.

For pseudovirus neutralization assays, 293T-ACE2 cells were seeded at 8,000 cells per well in white bottom 96-well plates in Dulbecco's modified Eagle's medium (DMEM) with 10% FBS and 1% P/S at 37 °C and 5% CO_2. 293T-ACE2 cells were treated 24 h post seeding with a final concentration of 5 μg/mL polybrene and mixtures containing 350 TCIU SARS-CoV-2 pseudovirus per well and antibody or nanobody treatments. The mixtures of antibody or nanobody and SARS-CoV-2 pseudovirus particles were incubated together for 1 h at 37 °C prior to incubation with 293T-ACE2 cells. At 48 h post infection, neutralizing activity was determined *via* chemiluminescence detection using a microplate reader (Molecular Devices SpectraMax set at 500 ms integration per well). Prior to chemiluminescence detection, luciferase substrate was added to each well following the manufacturer's protocol.

RESULTS

Evaluation of Spike Proteins for Inhibition Assay. The rapid *in vitro* inhibition assay (RIVIA) aims to simulate VNAs and obtain similar quantitative results in a much shorter time. An optimized RIVIA protocol should obtain a comparable inhibition efficacy with that obtained from a VNA for any antibody tested. By comparing the IC_{50} (half-maximal inhibitory concentration) obtained by the two assays, one can evaluate how successfully RIVIAs simulate VNAs.

To mimic the binding process between SARS-CoV-2 and human epithelial cells, we selected the recombinant extracellular domain (ECD) of the ACE2 receptor to be the capture probe in our RIVIA. While the S-ECD homotrimer is the natural form of the spike protein found on a virus, other forms of the spike proteins are also commercially available and need to be investigated. RBDs are the functional part of the spike proteins and are widely used in many existing assays[25−27] due to their high affinities to ACE2.[28] The S1 subunit contains the RBD and the N-terminal domain (NTD), and the full-length S-ECD monomer contains the S1 and S2 proteins. The S1 subunit and S-ECD monomer have more structural information than RBD while being more accessible to produce or purchase than the S-ECD homotrimer. It is critical to identify the optimal form of the spike protein for our assay.

We selected antibodies with different affinities and binding epitopes to ensure that our assay could be generalized and applied to a wide range of SARS-CoV-2 antibodies. We performed assays using animal-derived SARS-CoV-2 antibodies R001 (rabbit mAb). MM43 (mouse mAb), and MM57 (mouse mAb), and human-originated antibodies CB6 (human), AS35 (human), and CR3022 (human). All of the aforementioned antibodies were previously reported to have strong neutralizing efficacy against SARS-CoV-2. Non-neutralizing antibody D006 (humanized chimeric) was selected as a negative control. The antibody CR3022 was discovered in SARS-CoV patients but was shown to have cross-reactivity against the S1 subunit of SARS-CoV-2.[15,29] The neutralization efficacy of CR3022 toward SARS-CoV-2 is weak,[30,31] and we refer to it as a non-neutralizing antibody in this work.

In RIVIA, serial-diluted antibodies were incubated with four different forms of biotinylated SARS-CoV-2 S proteins for an hour. Then, each mixture was drawn into the microfluidic reactor with ACE2 immobilized on its inner surface. Spike proteins not fully inhibited then bind to ACE2 and are subsequently detected by Poly-HRP and a chemiluminescence substrate. A trade-off between complete incubation and short assay time exists. After some iterations, we have found that 1 h was sufficient for incubation, which provides high-quality results while keeping the total assay time (including incubation time and subsequent detection time) within 1.5 h.

At the same time, in Figure S2, we performed SARS-CoV-2 pVNAs with HEK 293 cells in a BSL-2 lab, with similar reagent arrangements for a side-by-side comparison. The results show that D006 is a non-neutralizing antibody, and CR3022 only demonstrated neutralization activity at extremely high concentrations. R001 is the strongest neutralizing antibody, followed by CB6. MM57, AS35, and MM43 display intermediate neutralizing activities.

https://doi.org/10.1021/acs.analchem.2c00062
Anal. Chem. 2022, 94, 4504−4512

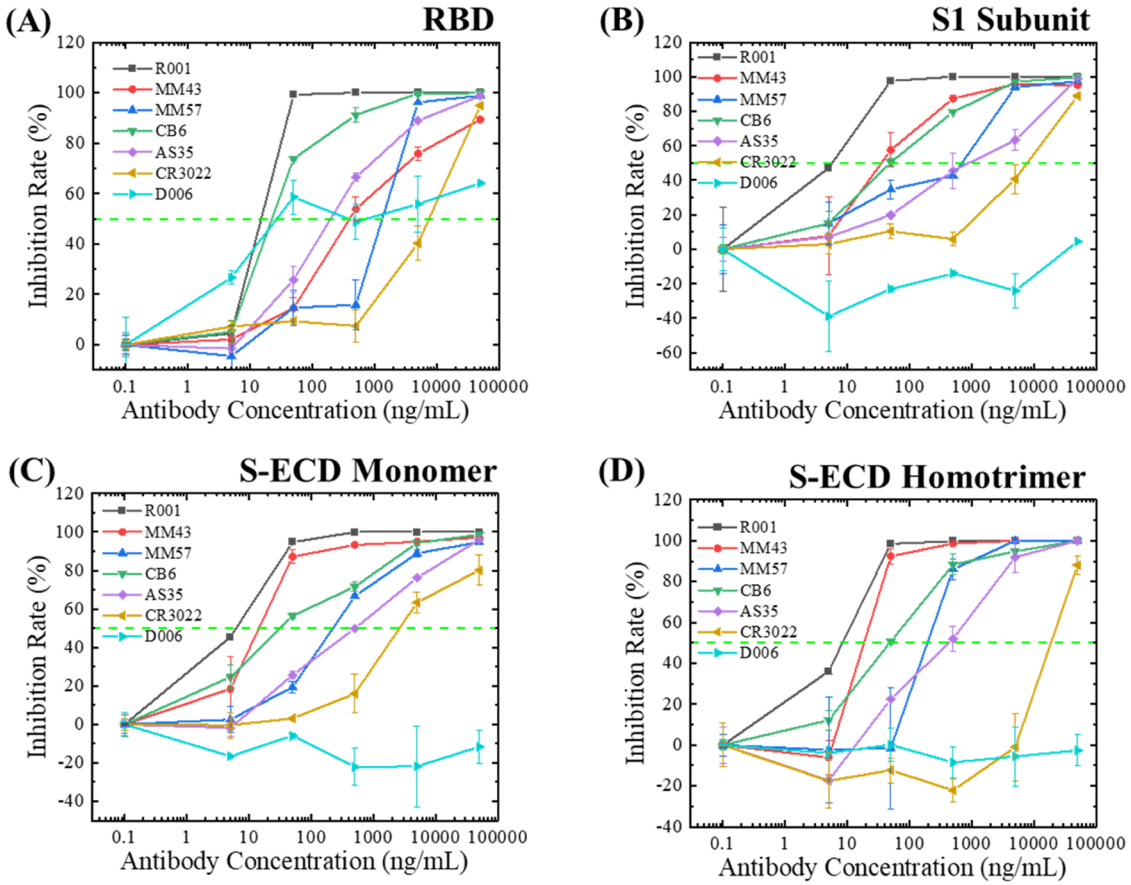

Figure 2. Optimization of RIVIA protocol. Tenfold serial-diluted antibodies starting at 50 μg/mL were tested with four different types of SARS-CoV-2 spike proteins. (A) RBD, (B) the S1 subunit, (C) the S-ECD monomer, and (D) the S-ECD homotrimer. Error bars are obtained by duplicate measurements. The dashed lines mark 50% inhibition. The corresponding IC_{50}s are tabulated in Table S3.

Figure 2A shows the results of RIVIA using RBD. R001 has the highest neutralizing efficacy, followed by CB6. AS35, MM43, and MM57 have similar neutralizing efficacy. MM43, for example, has an IC_{50} at 582 ng/mL. CR3022 is the weakest neutralizing antibody with an IC_{50} of 7527 ng/mL. However, unlike the pVNA results in Figure S2, RIVIA in this format overestimated the neutralizing efficacy of the weakest neutralizing antibody, CR3022, at low concentration. Moreover, the non-neutralizing antibody D006 can still inhibit the binding of RBD by more than 50% when the antibody concentration is higher than 50 ng/mL. This false-positive result could be caused by the small size of the RBD. The binding of D006 to a secondary epitope on RBD may also block the binding between RBD and ACE2.

Figure 2B shows the results of RIVIA using the S1 subunit. R001 remains as the strongest neutralizing antibody, followed by MM43 and CB6. CR3022 is the weakest neutralizing antibody with an IC_{50} at 7700 ng/mL. While D006 is correctly shown to be non-neutralizing in this assay format, the neutralizing efficacy of CR3022 is still overestimated. RIVIA using the S-ECD monomer (Figure 2C) is similar to RIVIA with the S1 subunit in Figure 2B. R001 is still the most effective neutralizing antibody, followed by MM43, CB6, MM57, and AS35. D006 is also correctly identified as non-neutralizing. However, the neutralizing efficacy of CR3022 is still overestimated. Figure 2D shows the results of RIVIA using the S-ECD protein homotrimer, which is similar to RIVIA with the S1 subunit and the S-ECD monomer in Figure 2B,C. CR3022 now lacks a neutralizing effect at low concentrations until it reaches a very high concentration (~20 000 ng/mL), which agrees with the pVNA finding in Figure S2. Note that for all antibodies, the baseline measurments (0 ng/mL) are marked as 0.1 ng/mL on the X-axis.

Comparing the results from the four RIVIA formats with those from the pVNA, RIVIA with RBD fails in terms of neutralizing efficacy. D006, a binding but non-neutralizing antibody, is incorrectly shown as a neutralizing antibody. RIVIA with the S1 subunit and S-ECD monomer can eliminate the false-positive results related to D006, but the use of both the S1 subunit and S-ECD monomer overestimates the neutralizing efficacy of CR3022 at low concentrations. In contrast, the S-ECD homotrimer is the optimal S protein for RIVIA. This is expected since the S-ECD homotrimer closely mimics the physiological configuration of the S protein on the virus surface.[32−34] D006 is correctly shown as a non-neutralizing antibody in this assay format, and CR3022 does not exhibit neutralizing abilities at lower concentrations (IC_{50} > 1000 ng/mL). All strong neutralizing antibodies can be easily distinguished from D006 and CR3022, and all of the IC_{50}s of antibodies are within the same order of magnitude as those measured by pVNAs. Therefore, RIVIA with the S-ECD homotrimer best simulates pVNAs.

Evaluation of Nanobodies for SARS-CoV-2. Nanobodies are single-domain proteins that can selectively bind to a specific antigen. Benefitted from their relatively small size, low molecular weight (~15 kD), and simple structure compared to

https://doi.org/10.1021/acs.analchem.2c00062
Anal. Chem. 2022, 94, 4504−4512

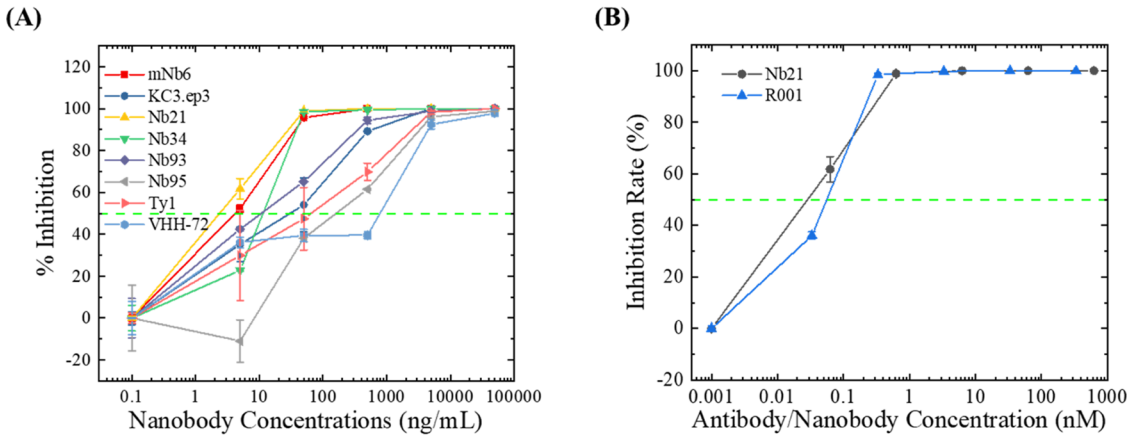

Figure 3. (A) Testing neutralizing nanobodies using RIVIA. Tenfold serial-diluted nanobodies were tested starting at 50 μg/mL. The dashed lines provide an estimate for half-neutralization. (B) Comparison of the neutralizing efficacy of the strongest antibody, R001, and the strongest nanobody, Nb21. Error bars are obtained by duplicate measurements. The dashed lines mark 50% inhibition. The corresponding IC_{50}s are tabulated in Table S4.

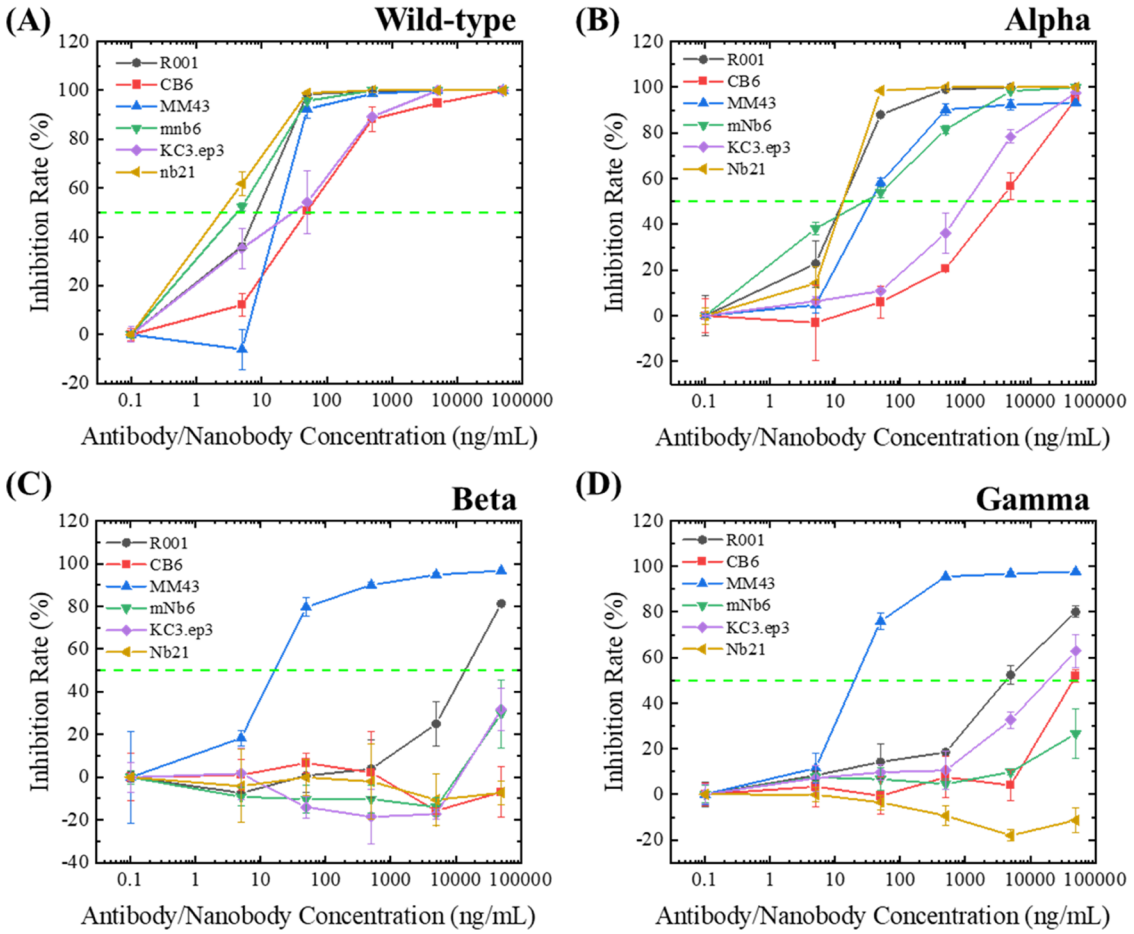

Figure 4. Testing the S-ECD homotrimer wild-type and three variants using RIVIA. Tenfold serial-diluted antibodies and nanobodies starting at 50 μg/mL were tested. (A) Wild-type, (B) α variant (B.1.1.7), (C) β variant (B.1.351), and (D) γ variant (P.1). Error bars are obtained by duplicate measurements. The dashed lines mark 50% inhibition. The corresponding IC_{50}s are tabulated in Table S5.

antibodies, nanobodies can be readily engineered and produced using standard approaches.[35] Genetically modified nanobodies have been increasingly used in research laboratories for imaging, biosensing, and clinical therapies in recent years.[36−38] Here, we tested a wide range of nanobody Fc fusions developed by groups from institutions worldwide to demonstrate that our system is applicable in evaluating the neutralizing efficacy of nanobodies for SARS-CoV-2. The assay protocol follows the optimized assay format determined in the Evaluation of Spike Proteins for Inhibition Assay section, where the S-ECD homotrimer is used.

https://doi.org/10.1021/acs.analchem.2c00062
Anal. Chem. 2022, 94, 4504−4512

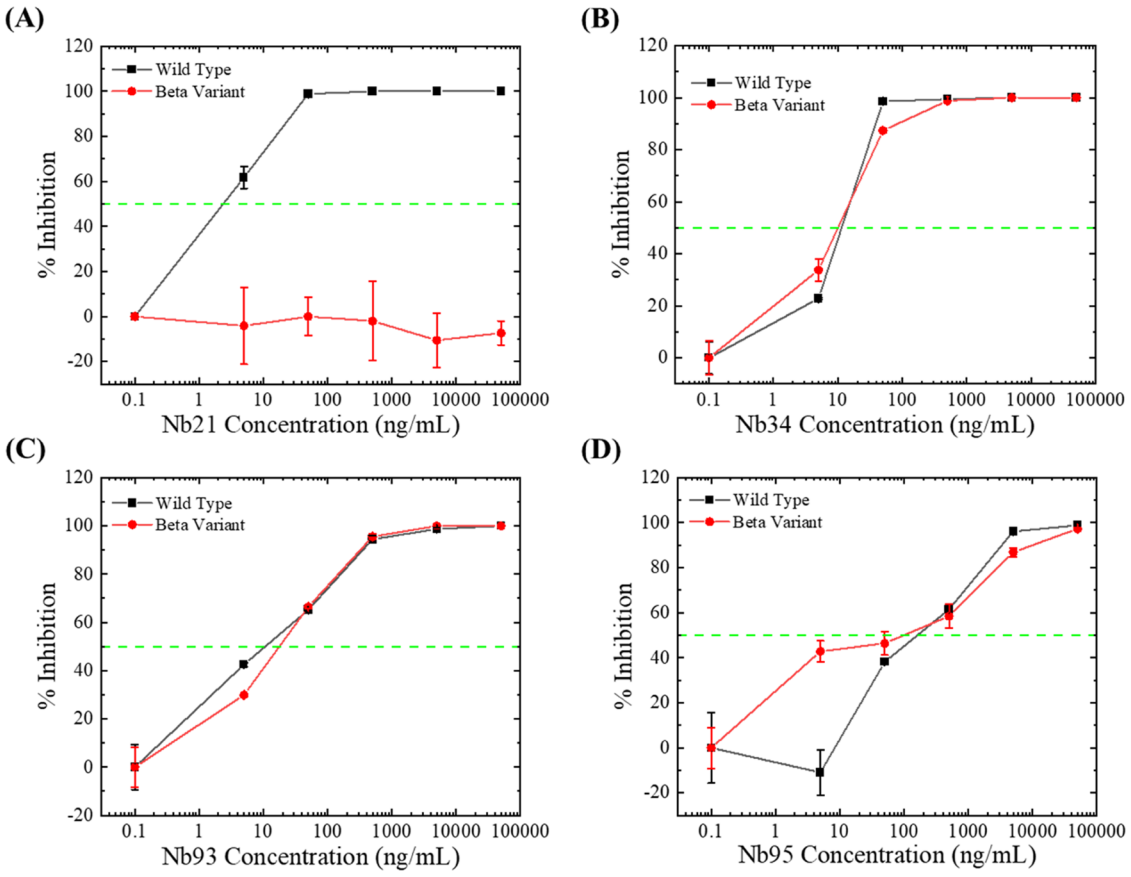

Figure 5. Screening of immune-evasive mutations on epitopes using RIVIA. Tenfold serial-diluted nanobodies starting at 50 μg/mL were tested. (A) Nb21, (B) Nb34, (C) Nb93, and (D) Nb95. Error bars are obtained by duplicate measurements. The dashed lines mark 50% inhibition. The corresponding IC_{50}s are tabulated in Table S6.

Figure 3A shows the inhibition of the S-ECD homotrimer using nanobody Fc fusions. Among the series of Nb nanobodies, Nb21 has the strongest neutralizing efficacy with an IC_{50} of 2 ng/mL, followed by mNb6 at 3 ng/mL. The second tier nanobodies are Nb93 and Nb34, both at 11 ng/mL, and KC3.ep3 at 22 ng/mL. Nb95 and VHH-72 are the weakest nanobodies at 149 and 790 ng/mL, respectively. The results agree relatively well with those from the pVNA shown in Figure S2, suggesting that RIVIA can also simulate the pVNA for nanobodies.

In Figure 3B, we compare the neutralizing efficacy of the strongest antibody with the strongest nanobody, which reveals that Nb21 has a lower IC_{50} and neutralizes more effectively than R001. Since the monoclonal antibody and nanobody Fc fusion have different molecular weights (R001 has a molecular weight of ~150 kD and Nb21 Fc fusion has a molecular weight of ~85 kD), molar concentrations are used in Figure 3B for comparison.

RIVIA for Evaluating SARS-CoV-2 Variants. Highly transmissible and immune-evasive variants pose a severe threat to the progress toward herd immunity worldwide. A fast and quantitative assay that can screen strongly neutralizing antibodies and nanobodies against emerging variants could help develop vaccines and therapies. Here, we tested a selected range of antibodies and nanobodies against three prevalent variants, α (B.1.1.7), β (B.1.351), and γ (P.1). Tenfold serial-diluted antibodies and nanobodies starting at 50 μg/mL were mixed with biotinylated S-ECD homotrimer variants at 140 ng/mL. The biotinylation of four S-ECD homotrimer variants (wild-type, α, β, and γ) was performed in one batch to minimize interbatch biotin concentration variations.

Figure S3 shows the binding of S-ECD homotrimer variants to ACE2 at the same concentration in the absence of antibodies. The wild-type has the lowest affinity of all, whereas the corresponding β and γ variants have increased affinity. The α variant has the highest affinity toward ACE2. This observation agrees well with recent reports that these prevalent variants have mutations that increase their affinity for ACE2.[39,40]

Figure 4A shows the RIVIA results for the wild-type. These results are extracted from Figures 2D and 3A. Figure 4B shows the RIVIA results for the α variant. This variant does not exhibit immune evasion, and thus it can be neutralized by the neutralizing antibodies or nanobodies at moderate concentrations. Nb21 and R001 are the strongest neutralizers, both having IC_{50} values of 13 ng/mL. MM43 has an IC_{50} of 47 ng/mL, and KC3.ep3 is at 1070 ng/mL. However, compared to the wild-type, the IC_{50}s of all of the antibodies and nanobodies, especially those of CB6 and KC3.ep3, increase significantly for the α variant, which is caused by the increased affinity of the α variant for ACE2.[39−41]

Figure 4C,D shows the RIVIA results for the β and γ variants, respectively. In contrast to the α variant, the β and γ variants show substantial immune evasion and share some immune-evasive mutations.[39,41] Therefore, many antibodies and nanobodies in this study fail to neutralize them effectively. Nb21, a strong neutralizing nanobody for the wild-type and α variant, loses most of its neutralizing efficacy. R001 can only

https://doi.org/10.1021/acs.analchem.2c00062
Anal. Chem. 2022, 94, 4504−4512

neutralize at a concentration above 50 000 ng/mL. All other antibodies and nanobodies (CB6, KC3.ep3, and mNb6) show little neutralizing efficacy. Only MM43 retains a strong neutralizing antibody with an IC_{50} of 16 ng/mL. Finally, comparing the results in Figure 4C,D, the β variant exhibits stronger immune evasion than the γ variant, which agrees with previous findings.[42,43]

Screening of Immune-Evasive Mutations on Variants. Antibodies and nanobodies with defined epitopes in the wild-type spike protein enable an analysis of the impacts of spike protein mutations in emerging variants on the binding of such affinity molecules. We used RIVIA to rapidly screen the impacts of evasive immune mutations on the binding of a panel of nanobodies to the S protein of different viral variants. This panel of previously reported nanobodies included those that bound to different epitopes on the S-ECD homotrimer.[20] We tested these nanobodies against the β variant, which has the highest efficiency of immune evasion among the three tested variants.[4142,43]

Again, we used the respective S-ECD homotrimer for the wild-type and β variants. Figure 5A compares the neutralization efficacy of Nb21 against the wild-type and β variant S-ECDs. While Nb21 is a strong neutralizing nanobody against the wild-type, it fails to neutralize the β variant. Figure 5B shows the neutralization effect of nanobody Nb34. Nb34 does not neutralize the wild-type as effectively as Nb21. However, it neutralizes the β variant with an IC_{50} of 10 ng/mL. As shown in Figure 5C,D, Nb93 and Nb95 neutralize the β variant with IC_{50} values of 18 and 44 ng/mL, respectively. Since all four tested Nbs bind to different epitopes, we infer that the mutations in the epitope of Nb21 may be related to the immune evasion ability of the β variant.

CONCLUSIONS

In this work, we demonstrated that RIVIA can simulate pVNAs for fast screening of antibodies and nanobodies. As compared to the pVNA, RIVIA has a number of advantages. RIVIA can be completed within 1.5 h, much shorter than 24−48 h typically required for the pVNA. Moreover, due to the microfluidic nature of the reactor, only 8 μL of low concentration reagent or sample is required. For example, only 70 ng/mL of the S protein is needed, while pVNAs require μg/mL levels. This leads to an estimate of less than $15 for one full RIVIA trial that includes six duplicated data points at six different concentrations. Although some *in vitro* assays such as lateral flow tests[44−46] can be used to rapidly evaluate the efficacy of neutralizing antibodies/nanobodies, they are unable to provide quantitative results.

In our work, we systematically studied various types of competitors, *i.e.*, RBD, the S1 subunit, the S-ECD monomer, and the S-ECD homotrimer, and found that the S-ECD homotrimer is the optimal choice, as it mimics the physiological configuration of the S protein on the virus surface. RBD, on the other hand, is prone to generating false-positive results (as shown in D006 in Figure 2A), which could be caused by the small size of RBD; the binding of an antibody on the secondary epitope of RBD may also block the binding between RBD and ACE2. This potential limitation of RBD is worth further investigation since RBD is still a popular competitor for *in vitro* SARS-CoV-2 neutralization assays.[25−27]

We also tested variants of the virus in our system and found that three variants, α, β, and γ, have higher affinities toward ACE2 than the wild-type. We tested the neutralizing efficacy of antibodies and nanobodies against them and found that both the β and γ variants are immune-evasive. Finally, we demonstrated another capability of RIVIA, *i.e.*, rapid screening of immune-evasive mutations using the nanobodies with known binding epitopes. We tested four nanobodies, Nb21, Nb34, Nb93, and Nb95, that bind to different classes of RBD epitopes. Since Nb21 loses neutralizing ability while the other three nanobodies remain effective, we infer that the immune-evasive mutations of the β and γ variants exist in the epitope recognized by Nb21. In the future, the concept of RIVIA will also be applied to the screening of neutralizing antibodies for other SARS-CoV-2 variants, such as Delta, Omicron BA.1, and Omicron BA.2. In addition, we found that the slope of the inhibition curves in RIVIA correlates with the binding affinity between the antibody and the spike protein. For example, as shown in Figure 2D, the slope of CB6 (nM level K_d) is smaller than that of R001 and MM43 (pM level K_d). These correlations will be investigated in our future research.

In a world where SARS-CoV-2 variants are emerging every now and then, RIVIA provides a more responsive approach for fast-filtering neutralizing antibodies that remain effective. Variants of S-ECD homotrimers used in RIVIA are easier and faster to develop and produce compared to the variants of pseudovirus. The fast response toward variants means that RIVIA can become a rapid and quantitative tool for the development of up-to-date effective neutralizing antibodies against the everchanging viruses.

ASSOCIATED CONTENT

Supporting Information

The Supporting Information is available free of charge at https://pubs.acs.org/doi/10.1021/acs.analchem.2c00062.

Assay protocols of RIVIA, pVNA results, affinity comparisons of S-ECD homotrimers of three variants and the wild-type, and tables of IC_{50} in different assay settings (PDF)

AUTHOR INFORMATION

Corresponding Authors

Peter M. Tessier − *Department of Biomedical Engineering, University of Michigan, Ann Arbor, Michigan 48109, United States; Department of Chemical Engineering, University of Michigan, Ann Arbor, Michigan 48109, United States; Department of Pharmaceutical Sciences and Biointerfaces Institute, University of Michigan, Ann Arbor, Michigan 48109, United States;* orcid.org/0000-0002-3220-007X; Email: ptessier@med.umich.edu

Xudong Fan − *Department of Biomedical Engineering, University of Michigan, Ann Arbor, Michigan 48109, United States;* orcid.org/0000-0003-0149-1326; Email: xsfan@umich.edu

Authors

Weishu Wu − *Department of Biomedical Engineering, University of Michigan, Ann Arbor, Michigan 48109, United States*

Xiaotian Tan − *Department of Biomedical Engineering, University of Michigan, Ann Arbor, Michigan 48109, United States;* orcid.org/0000-0001-5529-8092

Jennifer Zupancic − *Department of Chemical Engineering, University of Michigan, Ann Arbor, Michigan 48109, United*

https://doi.org/10.1021/acs.analchem.2c00062
Anal. Chem. 2022, 94, 4504−4512

States; Biointerfaces Institute, University of Michigan, Ann Arbor, Michigan 48109, United States

John S. Schardt − *Department of Chemical Engineering, University of Michigan, Ann Arbor, Michigan 48109, United States; Department of Pharmaceutical Sciences and Biointerfaces Institute, University of Michigan, Ann Arbor, Michigan 48109, United States*

Alec A. Desai − *Department of Chemical Engineering, University of Michigan, Ann Arbor, Michigan 48109, United States; Biointerfaces Institute, University of Michigan, Ann Arbor, Michigan 48109, United States*

Matthew D. Smith − *Department of Chemical Engineering, University of Michigan, Ann Arbor, Michigan 48109, United States; Biointerfaces Institute, University of Michigan, Ann Arbor, Michigan 48109, United States*

Jie Zhang − *Beijing Key Laboratory of Monoclonal Antibody Research and Development, Sino Biological Inc., Beijing 100176, China*

Liangzhi Xie − *Beijing Key Laboratory of Monoclonal Antibody Research and Development, Sino Biological Inc., Beijing 100176, China; Beijing Engineering Research Center of Protein and Antibody, Sinocelltech Ltd., Beijing 100176, China*

Maung Khaing Oo − *Optofluidic Bioassay, LLC, Ann Arbor, Michigan 48103, United States*

Complete contact information is available at: https://pubs.acs.org/10.1021/acs.analchem.2c00062

Author Contributions

○W.W. and X.T. contributed equally.

Notes

The authors declare the following competing financial interest(s): M. K. O. and X. F. are co-founders of and have an equity interest in Optofluidic Bioassay, LLC.

■ ACKNOWLEDGMENTS

This work was supported by the National Science Foundation [ECCS 2029484 to X.F.; CBET 1159943, 1605266, and 1813963 to P.M.T.; and Graduate Research Fellowship to M.D.S.], the National Institutes of Health (RF1AG059723 and R35GM136300 to P.M.T. and F32 GM137513 to J.S.S.), Biointerfaces Institute (to P.M.T.), and the Albert M. Mattocks Chair (to P.M.T.). The authors also thank the help from Corry Lin from Sino Biological.

■ REFERENCES

(1) Weiss, M.; Schwarzenberg, A.; Nelson, R.; Sutter, K. M.; Sutherland, M. D. *Global economic effects of COVID-19, Congressional Research Service*; 2020.

(2) WHO WHO Coronavirus (COVID-19) Dashboard. https://covid19.who.int/.

(3) Chen, P.; Nirula, A.; Heller, B.; Gottlieb, R. L.; Boscia, J.; Morris, J.; Huhn, G.; Cardona, J.; Mocherla, B.; Stosor, V.; et al. *N. Engl. J. Med.* **2021**, *384*, 229−237.

(4) Muruato, A. E.; Fontes-Garfias, C. R.; Ren, P.; Garcia-Blanco, M. A.; Menachery, V. D.; Xie, X.; Shi, P.-Y. *Nat. Commun.* **2020**, *11*, No. 4059.

(5) Bewley, K. R.; Coombes, N. S.; Gagnon, L.; McInroy, L.; Baker, N.; Shaik, I.; St-Jean, J. R.; St-Amant, N.; Buttigieg, K. R.; Humphries, H. E.; et al. *Nat. Protoc.* **2021**, *16*, 3114−3140.

(6) Nie, J.; Li, Q.; Wu, J.; Zhao, C.; Hao, H.; Liu, H.; Zhang, L.; Nie, L.; Qin, H.; Wang, M.; et al. *Emerging Microbes Infect.* **2020**, *9*, 680−686.

(7) Djaileb, A.; Charron, B.; Jodaylami, M. H.; Thibault, V.; Coutu, J.; Stevenson, K.; Forest, S.; Live, L. S.; Boudreau, D.; Pelletier, J. N. *ChemRxiv* **2020**, DOI: 10.26434/chemrxiv.12118914.v1.

(8) Van Elslande, J.; Houben, E.; Depypere, M.; Brackenier, A.; Desmet, S.; André, E.; Van Ranst, M.; Lagrou, K.; Vermeersch, P. *Clin. Microbiol. Infect.* **2020**, *26*, 1082−1087.

(9) Okba, N. M. A.; Müller, M. A.; Li, W.; Wang, C.; GeurtsvanKessel, C. H.; Corman, V. M.; Lamers, M. M.; Sikkema, R. S.; De Bruin, E.; Chandler, F. D.; et al. *Emerging Infect. Dis.* **2020**, *26*, 1478−1488.

(10) Tan, X.; Krel, M.; Dolgov, E.; Park, S.; Li, X.; Wu, W.; Sun, Y.-L.; Zhang, J.; Oo, M. K. K.; Perlin, D. S.; Fan, X. *Biosens. Bioelectron.* **2020**, *169*, No. 112572.

(11) Tan, X.; David, A.; Day, J.; Tang, H.; Dixon, E. R.; Zhu, H.; Chen, Y.-C.; Khaing Oo, M. K.; Shikanov, A.; Fan, X. *ACS Sens.* **2018**, *3*, 2327−2334.

(12) Tan, X.; Broses, L. J.; Zhou, M.; Day, K. C.; Liu, W.; Li, Z.; Weizer, A. Z.; Munson, K. A.; Oo, M. K. K.; Day, M. L.; Fan, X. *Lab Chip* **2020**, *20*, 634−646.

(13) Khaing Oo, M. K.; Fan, X. Optofluidic Diagnostics System. U.S. Patent US16/489,4202019.

(14) Shi, R.; Shan, C.; Duan, X.; Chen, Z.; Liu, P.; Song, J.; Song, T.; Bi, X.; Han, C.; Wu, L.; et al. *Nature* **2020**, *584*, 120−124.

(15) Yuan, M.; Wu, N. C.; Zhu, X.; Lee, C.-C. D.; So, R. T.; Lv, H.; Mok, C. K.; Wilson, I. A. *Science* **2020**, *368*, 630−633.

(16) Zupancic, J. M.; Desai, A. A.; Schardt, J. S.; Pornnoppadol, G.; Makowski, E. K.; Smith, M. D.; Kennedy, A. A.; de Mattos Barbosa, M. G.; Cascalho, M.; Lanigan, T. M.; Tai, A. W.; Tessier, P. M. *Cell Chem. Biol.* **2021**, *28*, 1379−1388.e7.

(17) Zupancic, J. M.; Schardt, J. S.; Desai, A. A.; Makowski, E. K.; Smith, M. D.; Pornnoppadol, G.; Garcia de Mattos Barbosa, M.; Cascalho, M.; Lanigan, T. M.; Tessier, P. M. *Adv. Ther.* **2021**, *4*, No. 2100099.

(18) Hanke, L.; Perez, L. V.; Sheward, D. J.; Das, H.; Schulte, T.; Moliner-Morro, A.; Corcoran, M.; Achour, A.; Hedestam, G. B. K.; Hällberg, B. M. *Nat. Commun.* **2020**, *11*, No. 4420.

(19) Wrapp, D.; De Vlieger, D.; Corbett, K. S.; Torres, G. M.; Wang, N.; Van Breedam, W.; Roose, K.; van Schie, L.; COVID, V.-C.; Team, R.; et al. *Cell* **2020**, *181*, 1004−1015. e15.

(20) Xiang, Y.; Nambulli, S.; Xiao, Z.; Liu, H.; Sang, Z.; Duprex, W. P.; Schneidman-Duhovny, D.; Zhang, C.; Shi, Y. *Science* **2020**, *370*, 1479−1484.

(21) Tan, X.; Oo, M. K. K.; Gong, Y.; Li, Y.; Zhu, H.; Fan, X. *Analyst* **2017**, *142*, 2378−2385.

(22) Crawford, K. H. D.; Eguia, R.; Dingens, A. S.; Loes, A. N.; Malone, K. D.; Wolf, C. R.; Chu, H. Y.; Tortorici, M. A.; Veesler, D.; Murphy, M.; et al. *Viruses* **2020**, *12*, No. 513.

(23) Zupancic, J. M.; Desai, A. A.; Schardt, J. S.; Pornnoppadol, G.; Makowski, E. K.; Smith, M. D.; Kennedy, A. A.; de Mattos Barbosa, M. G.; Cascalho, M.; Lanigan, T. M.; Tai, A. W.; Tessier, P. M. *Cell Chem. Biol.* **2021**, *28*, 1379−1388.e7.

(24) Schardt, J. S.; Pornnoppadol, G.; Desai, A. A.; Park, K. S.; Zupancic, J. M.; Makowski, E. K.; Smith, M. D.; Chen, H.; Garcia de Mattos Barbosa, M.; Cascalho, M.; Lanigan, T. M.; Moon, J. J.; Tessier, P. M. *Sci. Rep.* **2021**, *11*, No. 20738.

(25) Tan, C. W.; Chia, W. N.; Qin, X.; Liu, P.; Chen, M. I.-C.; Tiu, C.; Hu, Z.; Chen, V. C.-W.; Young, B. E.; Sia, W. R.; et al. *Nat. Biotechnol.* **2020**, *38*, 1073−1078.

(26) Abe, K. T.; Li, Z.; Samson, R.; Samavarchi-Tehrani, P.; Valcourt, E. J.; Wood, H.; Budylowski, P.; Dupuis, A. P.; et al. *JCI Insight* **2020**, *5*, No. e142362.

(27) Byrnes, J. R.; Zhou, X. X.; Lui, I.; Elledge, S. K.; Glasgow, J. E.; Lim, S. A.; Loudermilk, R. P.; Chiu, C. Y.; Wang, T. T.; Wilson, M. R.; et al. *MSphere* **2020**, *5*, No. e00802-20.

(28) Tai, W.; He, L.; Zhang, X.; Pu, J.; Voronin, D.; Jiang, S.; Zhou, Y.; Du, L. *Cell. Mol. Immunol.* **2020**, *17*, 613−620.

(29) Joyce, M. G.; Chen, W.-H.; Sankhala, R.; Hajduczki, A.; Thomas, P. V.; Choe, M.; Martinez, E.; Chang, W.; Peterson, C. E.; Morrison, E. B.; et al. *Cell Rep.* **2021**, *37*, No. 110143.

(30) Tian, X.; Li, C.; Huang, A.; Xia, S.; Lu, S.; Shi, Z.; Lu, L.; Jiang, S.; Yang, Z.; Wu, Y.; Ying, T. *Emerging Microbes Infect.* **2020**, *9*, 382−385.
(31) Zhou, G.; Zhao, Q. *Int. J. Biol. Sci.* **2020**, *16*, 1718.
(32) Delmas, B.; Laude, H. *J. Virol.* **1990**, *64*, 5367−5375.
(33) Vinson, V. *Science* **2020**, *36 7*, 1207.3−1207.
(34) Fenwick, C.; Turelli, P.; Pellaton, C.; Farina, A.; Campos, J.; Raclot, C.; Pojer, F.; Cagno, V.; Nusslé, S. G.; D'Acremont, V.; Jan Fehr7, M. P.; Pantaleo, G.; Trono, D.; et al. *Sci. Transl. Med.* **2021**, *13*, No. eabi8452.
(35) McMahon, C.; Baier, A. S.; Pascolutti, R.; Wegrecki, M.; Zheng, S.; Ong, J. X.; Erlandson, S. C.; Hilger, D.; Rasmussen, S. G.; Ring, A. M.; Manglik, A.; Kruse, A. C. *Nat. Struct. Mol. Biol.* **2018**, *25*, 289−296.
(36) Guo, K.; Wustoni, S.; Koklu, A.; Díaz-Galicia, E.; Moser, M.; Hama, A.; Alqahtani, A. A.; Ahmad, A. N.; Alhamlan, F. S.; Shuaib, M.; et al. *Nat. Biomed. Eng.* **2021**, *5*, 666−677.
(37) Virant, D.; Traenkle, B.; Maier, J.; Kaiser, P. D.; Bodenhöfer, M.; Schmees, C.; Vojnovic, I.; Pisak-Lukáts, B.; Endesfelder, U.; Rothbauer, U. *Nat. Commun.* **2018**, *9*, No. 930.
(38) Cortez-Retamozo, V.; Backmann, N.; Senter, P. D.; Wernery, U.; De Baetselier, P.; Muyldermans, S.; Revets, H. *Cancer Res.* **2004**, *64*, 2853−2857.
(39) Harvey, W. T.; Carabelli, A. M.; Jackson, B.; Gupta, R. K.; Thomson, E. C.; Harrison, E. M.; Ludden, C.; Reeve, R.; Rambaut, A.; Peacock, S. J.; Robertson, D. L. *Nat. Rev. Microbiol.* **2021**, *19*, 409−424.
(40) Kidd, M.; Richter, A.; Best, A.; Cumley, N.; Mirza, J.; Percival, B.; Mayhew, M.; Megram, O.; Ashford, F.; White, T.; Moles-Garcia, E.; Crawford, L.; Bosworth, A.; Atabani, S. F.; Plant, T.; McNally, A. *J. Infect. Dis.* **2021**, *223*, 1666−1670.
(41) Ramanathan, M.; Ferguson, I. D.; Miao, W.; Khavari, P. A. *Lancet Infect. Dis.* **2021**, *21*, No. 1070.
(42) Hoffmann, M.; Arora, P.; Groß, R.; Seidel, A.; Hörnich, B. F.; Hahn, A. S.; Krüger, N.; Graichen, L.; Hofmann-Winkler, H.; Kempf, A.; et al. *Cell* **2021**, *184*, 2384−2393.e12.
(43) Wang, P.; Nair, M. S.; Liu, L.; Iketani, S.; Luo, Y.; Guo, Y.; Wang, M.; Yu, J.; Zhang, B.; Kwong, P. D.; et al. *Nature* **2021**, *593*, 130−135.
(44) Ragnesola, B.; Jin, D.; Lamb, C. C.; Shaz, B. H.; Hillyer, C. D.; Luchsinger, L. L. *BMC Res. Notes* **2020**, *13*, No. 372.
(45) Wang, J. J.; Zhang, N.; Richardson, S. A.; Wu, J. V. *Expert Rev. Mol. Diagn.* **2021**, *21*, 363−370.
(46) Kongsuphol, P.; Jia, H.; Cheng, H. L.; Gu, Y.; Shunmuganathan, B. D.; Chen, M. W.; Lim, S. M.; Ng, S. Y.; Tambyah, P. A.; Nasir, H.; et al. *Commun. Med.* **2021**, *1*, No. 46.

https://doi.org/10.1021/acs.analchem.2c00062
Anal. Chem. 2022, 94, 4504−4512